

Geophysical analysis of the Curral Homocline and Moeda Syncline junction, Quadrilátero Ferrífero, MG

Ramon Danilo de Souza*¹, Maria Sílvia Carvalho Barbosa², Issamu Endo², Luis Artur Souza Oliveira², Raissa Felix de Alvarenga², Paola Pepino Tarabini², Mateus Malaquias Nascimento², Vitória Rodrigues França² and Joney Justo da Silva²;
¹ Federal University of Ouro Preto.

Copyright 2021, SBGf - Sociedade Brasileira de Geofísica

This paper was prepared for presentation during the 17th International Congress of the Brazilian Geophysical Society held in Rio de Janeiro, Brazil, 16-19 August 2021.

Contents of this paper were reviewed by the Technical Committee of the 17th International Congress of the Brazilian Geophysical Society and do not necessarily represent any position of the SBGf, its officers or members. Electronic reproduction or storage of any part of this paper for commercial purposes without the written consent of the Brazilian Geophysical Society is prohibited.

Abstract

The Quadrilátero Ferrífero (QFe) has been intensively studied over the last few decades, given its structural complexity and economic importance. For the study, an analysis of geophysical data (magnetometry) of the northwest portion of the QFe was carried out. The study area has an intense structural complexity and is considered a key to better understanding the various and controversial tectonic models proposed for the QFe region. The magnetometry aerial survey databases were compiled and processed for the production of several thematic geophysical maps which were treated in a quali-quantitative analysis, allowing extracting relevant information from subsurface rocks, through 2D inverted profiles and 3D in-depth views of the selected area. Euler deconvolution was performed in a regular grid of profiles in NW-SE direction and profiles coincident with the mapped geological ones. The inverted magnetometric profiles characterized very well the planar structures at the investigated depths and allowed the 3D view of the main fault zones (Curral and Mário Campos faults) that outcrop in the area. The comparison of the results obtained with the adopted model of tectonic development for the region of the junction between the Curral Homocline and the Moeda Syncline is consistent with the structures observed in this study.

Introduction

The Quadrilátero Ferrífero (QFe) is located in the south-central region of the state of Minas Gerais, on the southern edge of the São Francisco Craton, in the foreland domain of the Mineiro Belt (Alkmim & Marshak 1998). The main units that compose it are the rocks of the Rio das Velhas, Minas and Estrada Real Supergroups, the basal metamorphic complexes and a substantial volume of Archean to Paleoproterozoic granitoids (Endo et al. 2020). The study area (Figure 1) is the junction between the Curral Homocline and the Moeda Syncline and has a high structural complexity.

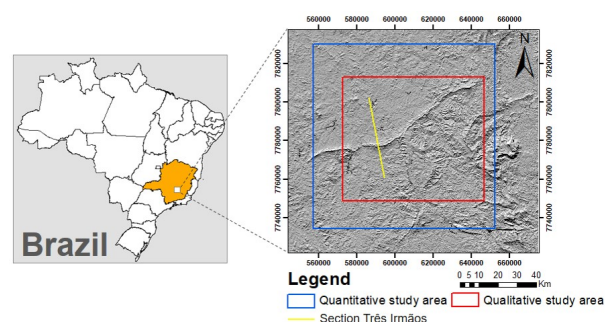


Figure 1 – Study area location map.

The tectonic-stratigraphic elements surveyed by Endo et al. (2005) for the study area (Figure 2) are articulated through a northeast-verging nappes tectonics where the units of the Rio das Velhas Supergroup occupy the core of an allochthonous recumbent megafold called Nappe Curral (Endo et al. 2005).

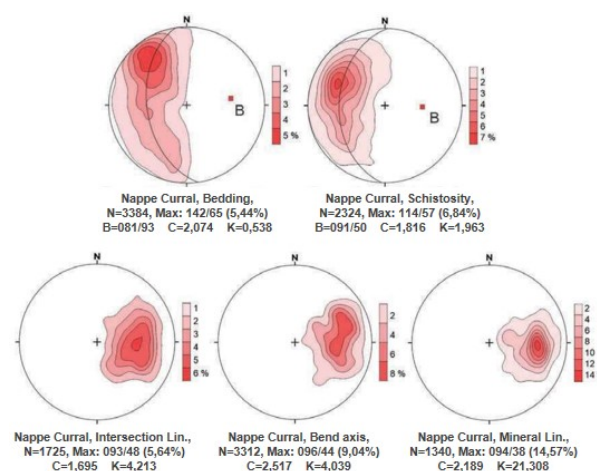


Figure 2 – Tectonic-stratigraphic elements collected by Endo et al. (2005).

The transport of the Nappe Curral took place over a basal detachment surface located over the Bonfim Complex gneisses, where the trace of this surface in the south of the Serra do Curral and west of the Moeda Syncline follows the contact of the Bonfim Gneiss with the supracrustal rocks (Endo et al. 2005). The nappe front is typified by the Curral thrust fault that emerges at the interface between the Sabará Group and the Minas Supergroup, in the north of the Serra do Curral (Figure 3, structure 5).

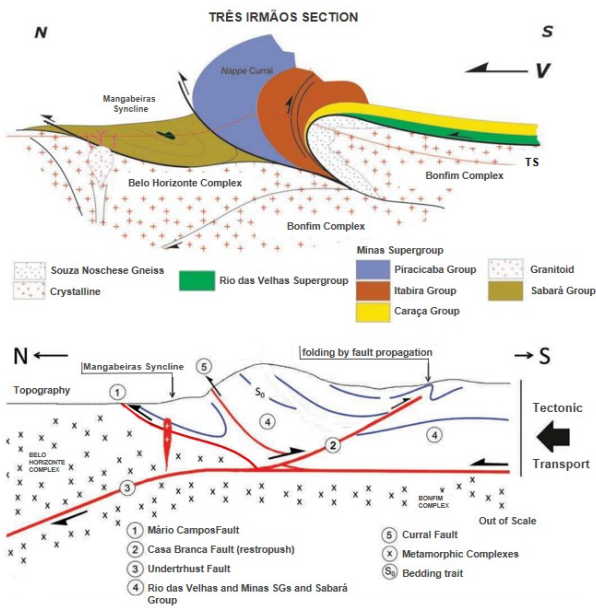


Figure 3 – Model of tectonic evolution proposed by Endo et al 2005, Três Irmãos section (location see figure 1).

The Mangabeiras Syncline with an axial trace subparallel to the Curral Fault trace is the result of the advance of Nappe Curral over the Sabará Group. In this context, a typical arrangement of thrust faults emerges delimiting the foreland syncline called “out-of-syncline thrusts”, which are faults that are molded around the syncline, one with synthetic kinematics and the other antithetical. The synthetic fault is represented by the Mário Campos thrust fault (Figure 3 structure 1). The antithetic fault was not observed on the surface; however, the movement effect of antithetic masses is manifested through kink-type folds verging to S-SW. The back-thrust faults (Figure 3 structure 2) are caused by the process of mass flow reversal to the south in the northern third of the Moeda Syncline, evidenced by the reversal of counterclockwise to clockwise vorticity on the W flank, and from clockwise to counterclockwise, on the E flank (Endo et al. 2020).

The late-tectonic phase of the ascension of crystalline basement blocks was accompanied by the intrusion of several small granitoid bodies into the rocks of the Sabará Group, positioned along the axial direction of the Mangabeiras Syncline (Noce 1995, Endo et al. 2019a,b). In the genesis of the granitoids, the hypothesis of partial melting of the crust in response to the interaction between the blocks of the Belo Horizonte and Bonfim metamorphic complexes through an underthrust fault is considered (Figure 3 structure 3; Endo et al. 2005).

The study aimed viewing in depth the internal structuring of the Curral Homocline and Moeda Syncline junction, specifically the underthrust fault (Figure 3 structure 3), proposed by Endo et al. (2005 and 2020).

Method

The tectono-structural geophysical analysis is based on the interpretation of geophysical products such as 2D

thematic maps (Telford et al. 1990, Kearey et al. 2009) and the inversion of 2D data and 3D views. Therefore, several thematic magnetometric maps were generated (Figure 4), using the Oasis Montaj software. The data were interpolated employing the minimum curvature method in a regular grid with 700m cells, generating the thematic map of Anomalous Field (CA). Subsequently, the MAGMAP – Analytic Signal routine was performed, enabling the elaboration of the Analytic Signal Amplitude thematic map (ASA). By applying filters and performing the MAGMAP routine, it was possible to generate the other thematic maps, vertical gradient of first order (Dz) and first order horizontal gradients in X (Dx) and Y (Dy) for the anomalous field data and the vertical gradient of first order of analytical signal amplitude (DASA).

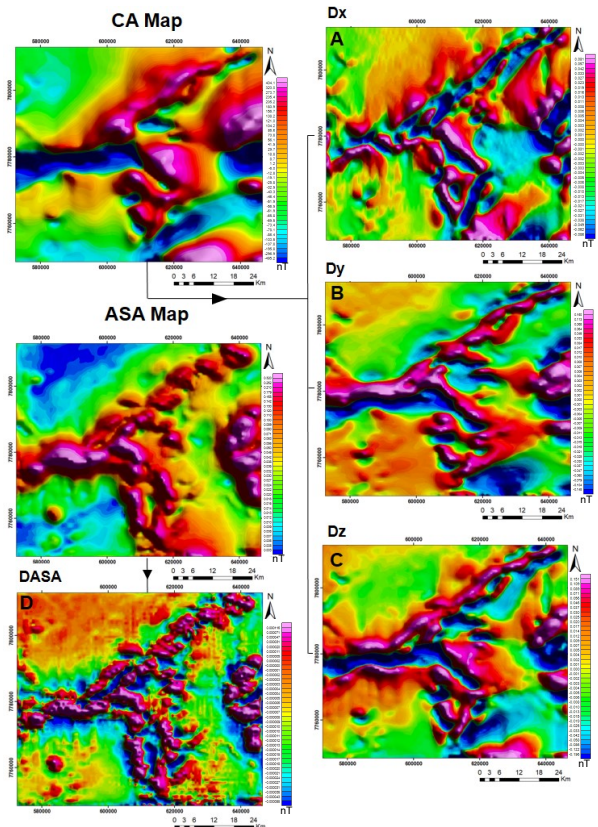


Figure 4 – Magnetometric thematic maps. (A) map of first order horizontal gradient in X (Dx) for the anomalous field data. (B) map of first order horizontal gradients in Y (Dy) for the anomalous field data. (C) map of first order vertical gradients (Dz) for the anomalous field data. (D) map of first order vertical gradient of analytical signal amplitude (DASA).

The quantitative analysis consisted in inverting the magnetometry data, applying the Euler deconvolution (Thompson 1982, Reid et al. 1990) in a regular grid with 24 profiles, 2.5 km equidistant, 62 km long and NW-SE direction (Figure 5). The inversion of geophysical profiles coincident with the geological ones performed by Endo et al. (2005) was also carried out, employing the ArcGIS v.10.3, Oasis Montaj v.8.4 and Euldeph v.1.00 softwares

from the School of Geosciences – School of the Witwatersrand.

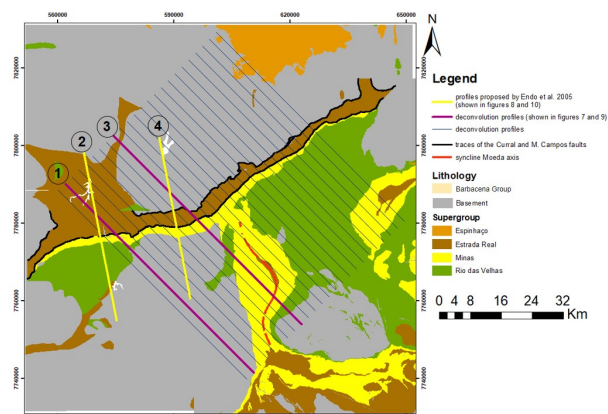


Figura 5 – Simplified geological map of the Quadrilátero Ferrífero indicating the locations of the profiles shown in figures 7, 8, 9 and 10.

The Euldeph software (Thompson 1982) employs the height of the data survey and processes them by analyzing the relationship between wavelength and amplitude of the signals, in order to estimate the depth of the average top of the bodies that generated the magnetometric anomalies. To refine the results of this process, the operator determines the parameters that best fit the geological situation investigated, such as the estimated maximum depth, structural index and window size. The parameters applied to this study were structural index equal to 1 (planar structures) and window size 11. The results obtained from the Euler deconvolution profiles were interpolated by the kriging method, thus obtaining a 3D view of the depth of the average top of the bodies that generated the magnetometric anomalies.

Results

The study of magnetic lineaments presented a preferred E-W pattern (Figure 6), direction that was consistent with the penetrative grids of the fold axis, mineral lineation and intersection lineation (see Figure 2) observed by Endo et al. (2005).

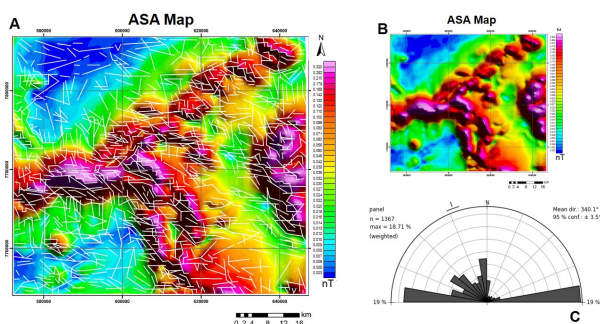


Figura 6 – Magnetometric Lineaments. (A) ASA map with the observed lineaments. (B) ASA map. (C) rosette diagram of the preferred directions of the magnetometric lineaments.

The two-dimensional deconvolution profiles presented here are distributed along the Curral Fault trace in the western and central portions of the structure. Profiles 1 and 3 derive from the regular grid described above and profiles 2 and 4 coincide with the geological ones made by Endo et al. (2005) (Figure 5). All four profiles intersect the Curral Fault and profiles 3 and 4 cover the Mário Campos Fault trace in its western portion as well.

The profile 1 (Figure 7) has a maximum depth of approximately 26000 meters and enables tracing features such as the Curral Fault structures (Figure 7D, in light blue), the back-thrust faults (Figure 7D, in green), the upper detachment of the Curral Bonfim Anticline (Figure 7D, in beige), the detachment of the Nappe Curral over the basement (Figure 7D, in dark blue), the structuring of the W flank of the Moeda Syncline (Figure 7D, in brown) and a NW dip structure that reaches a depth of approximately 20,000 meters (Figure 7D, depicted in red). Analyzing the model presented by Endo et al. (2005), this deeper structure can be interpreted as the underthrust fault that this work investigates.

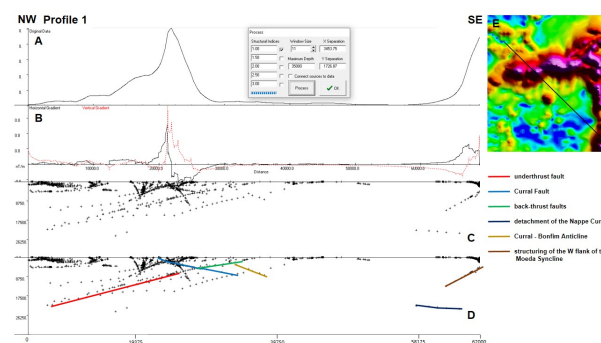


Figura 7 – Profile 1 two-dimensional. (A) Magnetometric signal and parameters used in the process of inversion. (B) Horizontal and vertical gradients. (C) Average top anomaly responses. (D) Inversion of profile 1 interpreted. (E) ASA map with the location of profile 1.

The profile 2 (Figure 8) has a maximum depth of approximately 25000 meters and, similarly, allows viewing the Curral Fault structures, the back thrust faults, the displacement of the Nappe Curral over the basement and the underthrust fault, which in this profile specifically reaches the depth of approximately 24,000 meters. The emergence of a new structure with SE dip observed in Figure 8D in yellow is noteworthy.

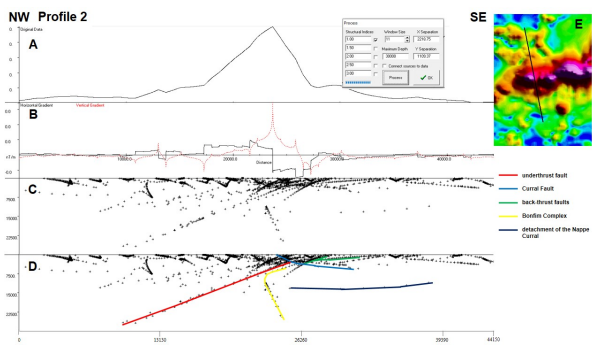


Figura 8 – Profile 2 two-dimensional. (A) Magnetometric signal and parameters used in the process of inversion. **(B)** Horizontal and vertical gradients. **(C)** Average top anomaly responses. **(D)** Inversion of profile 2 interpreted. **(E)** ASA map with the location of profile 2.

The profile 3 (Figure 9) does not have a depth as high as the profiles presented above, with a maximum of approximately 13000 meters. In this profile, in addition to the structures of the Curral Fault, back-thrust faults and the basal displacement of the Nappe Curral, the Mário Campos Fault (Figure 9D, represented in lilac) and the structuring of the Moeda Syncline may be observed. The depth reached by this profile was not enough to characterize the underthrust fault; however, more superficial structures with an attitude similar to the investigated fault are portrayed in the profile and were interpreted as a more superficial product of the interaction between the Belo Horizonte and Bonfim Metamorphic Complexes.

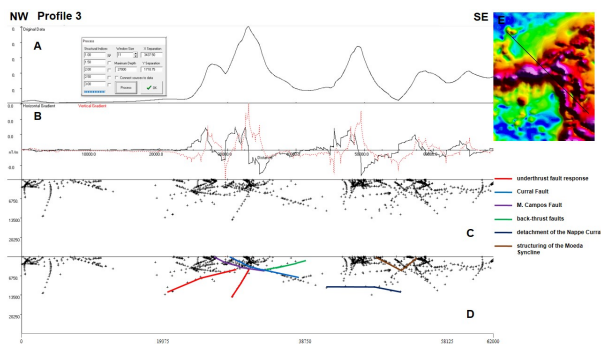


Figura 9 – Profile 3 two-dimensional. (A) Magnetometric signal and parameters used in the process of inversion. **(B)** Horizontal and vertical gradients. **(C)** Average top anomaly responses. **(D)** Inversion of profile 3 interpreted. **(E)** ASA map with the location of profile 3.

The profile 4 (Figure 10) has a maximum depth of 30000 meters and allows observing the structures of the Curral Fault, Mário Campos Fault, the back thrust faults and the underthrust fault (which specifically in this profile reaches a depth of approximately 13000 meters). In addition to this structuring, one can also infer a structure resulting from the involvement of the Bonfim Metamorphic Complex in the core of Nappe Curral (Figure 10F).

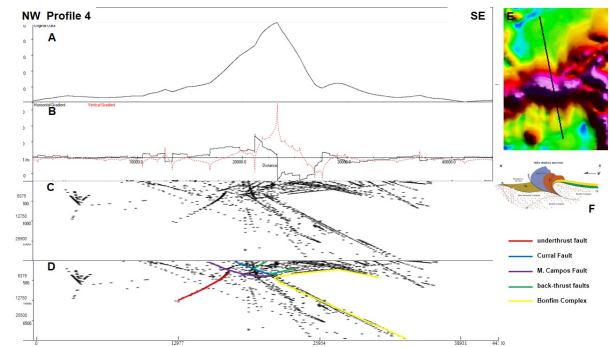


Figura 10 – Profile 4 two-dimensional. (A) Magnetometric signal and parameters used in the process of inversion. **(B)** Horizontal and vertical gradients. **(C)** Average top anomaly responses. **(D)** Inversion of profile 4 interpreted. **(E)** ASA map with location of profile 4. **(F)** Tectonic development model proposed by Endo et al. (2005).

The profile 4 presented the best response in the inversion process when compared to the tectonic development model proposed by Endo et al. (2005). Considering that the two-dimensional profiles present a vertical exaggeration in the Euldeph software, Figure 11 shows the proposed model and profile 4 in a three-dimensional view.

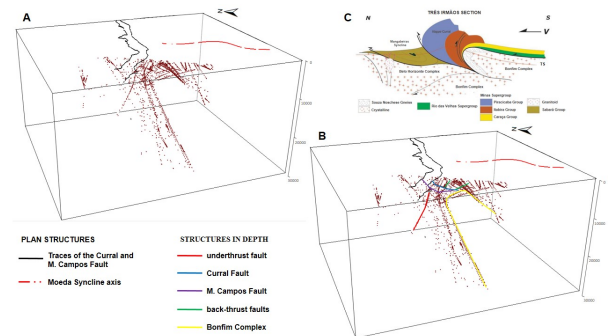


Figura 11 – Three-dimensional view of profile 4. (A) 3D view of profile 4 with Curral and Mário Campos faults traced and the identification of the Moeda Syncline axis. **(B)** 3D view of profile 4 with the interpretation of the structures of the Curral and Mário Campos Faults, the back-thrust faults, the underthrust fault and the involvement of the Bonfim Complex in the Nappe Curral core. **(C)** Três Irmãos Section proposed for the location, TS – Topographic Surface (Endo et al. 2005).

From this analysis, it is noted that the arrangement of the structures represented in the profile figures is consistent with the proposed structural arrangement for the region of the junction between the Curral Homocline and Moeda Syncline, altogether, there is a high probability of the existence of the underthrust fault proposed by Endo et al. (2005)

The three-dimensional model represented very well the region of the Curral and Mário Campos Faults (Figure 12)

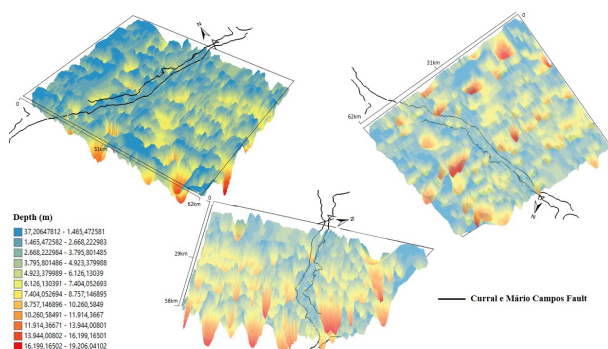


Figura 12 – Interpolated three-dimensional model with identification of the traces of the Curral and Mário Campos Fault.

In the region where the Curral and Mário Campos Faults are located, the identified average anomaly tops are more superficial, since the faults in this area outcrop and are mappable. From the identified fault traces, to the south, the represented average anomaly tops are deeper characterizing the typical expected geometry for the thrust faults.

The three-dimensional model in Figure 12 was not categorical in identifying the underthrust fault. Since the Quadrilátero Ferrífero has a high structural complexity and the method used to invert the data calculates the average top of the bodies that generate the anomalies. Resulting in a very high variability of the profile data generated for the region.

Conclusions

The magnetometric analysis allowed viewing the evidential structures of the underthrust fault, in addition to other structures that make up the tectonic development model proposed by Endo et al. (2005). For instance, the arrangement of the Curral and Mário Campos Faults, the back thrust faults and the structuring of the underthrust fault with the involvement of the Bonfim Metamorphic Complex in the Nappe Curral core.

The profile 4, coinciding with the Três Irmãos section, had the most coherent result with the adopted tectonic development model, as it characterized all the structures described in the model.

The three-dimensional magnetometric model represented the region of the Curral and Mário Campos Faults very well, characterizing the geometry of the thrust faults. However, they did not help in the modeling of the investigated underthrusting surface, due to the structural complexity of the Quadrilátero Ferrífero.

Acknowledgments

The authors would like to thank Society of Applied Geophysics (Sociedade de Geofísica Aplicada - SGA) and the Federal University of Ouro Preto for the opportunity to elaborate this work.

References

ALKMIM F. F. & MARSHAK S. 1998. Transamazonian Orogeny In the Southern São Francisco Craton Region Minas Gerais, Brazil: evidence for Paleoproterozoic collisional and collapse in the Quadrilátero Ferrífero. *Precambrian Research*, 90: 29-58.

ENDO I., OLIVEIRA A. H., PERES G. G., GUIMARÃES M. L. V., LAGOEIRO L. E., MACHADO R., ZAVAGLIA G., ROSAS C. F., MELO R. J.. 2005. Nappe Curral: Uma megaestrutura alóctone do Quadrilátero Ferrífero e controle da mineralização. In: X Simpósio Nacional de Estudos Tectônicos / IV International Symposium on Tectonics. Curitiba. Boletim de Resumos Expandidos, p.: 279-282.

ENDO I., GALBIATTI H. F., DELGADO C. E. R., OLIVEIRA M. M. F. DE, ZAPPAROLI A. DE C., MOURA L. G. B. DE, PERES G. G., OLIVEIRA A. H. DE, ZAVAGLIA G., DANDERFER F. A., GOMES C. J. S., CARNEIRO M. A., NALINI JR. H. A., CASTRO P. DE T. A., SUITA M. T. DE F., TAZAVA E., LANA C. DE C., MARTINS-NETO M. A., MARTINS M. DE S., FERREIRA F. A., FRANCO A. P., ALMEIDA L. G., ROSSI D. Q., ANGELI G., MADEIRA T. J. A., PIASSA L. R. A., MARIANO D. F., CARLOS D. U.. 2019a. Mapa Geológico do Quadrilátero Ferrífero, Minas Gerais, Brasil. Escala 1:150.000: Uma celebração do cinquentenário da obra de Dorr (1969).Ouro Preto, Departamento de Geologia da Escola de Minas – UFOP - Centro de Estudos Avançados do Quadrilátero Ferrífero: www.qfe2050.ufop.br.

ENDO I., DELGADO C. E. R. OLIVEIRA M. M. F. DE, ZAPPAROLI A. DE C., CARLOS D. U., GALBIATTI H. F., CASTRO P. DE T. A., SUITA M. T. DE F., BARBOSA M. S. C., LANA C. E., MOURA L. G. B. DE. 2019b. Estratigrafia e Arcabouço Estrutural do Quadrilátero Ferrífero: Nota Explicativa do Mapa Geológico do Quadrilátero Ferrífero, Minas Gerais, Brasil. Escala 1:150.000. Ouro Preto, Departamento de Geologia da Escola de Minas – UFOP - Centro de Estudos Avançados do Quadrilátero Ferrífero: www.qfe2050.ufop.br.

ENDO, I, MACHADO R., GALBIATTI, H. F., ROSSI, D. Q., ZAPPAROLI, A. C., DELGADO, C. E. R., CASTRO, P. T. A., OLIVEIRA, M. M. F.. 2020. Estratigrafia e evolução estrutural do Quadrilátero Ferrífero. In: Quadrilátero Ferrífero: Avanços do conhecimento nos últimos 50 anos (Organizadores: Castro, P.T.A., Endo, I., Gandini, A. L.). Editado por 3i Editora.

KEAREY P., BROOKS M. & HILL I. 2009. Geofísica de Exploração. Tradução de Coelho M. C. M., São Paulo. 262p..

NOCE C. M.. 1995. Geocronologia dos eventos magmáticos, sedimentares e metamórficos na região do Quadrilátero Ferrífero, Minas Gerais. Instituto de Geociências da Universidade de São Paulo, São Paulo, Tese de Doutorado, 129 p..

TELFORD W. M., GELDART L.P., SHERIFF R.E. 1990. Applied Geophysics. Cambridge, Cambridge University Press. 770p..

THOMPSON, D. T. 1982. EULDPH: A new technique for making computer-assisted.

REID A. B., ZHANG. C., MUSHAYANDEBVU M. F., FAIRHEAED J. D., ODEGARD M. E., 1990. Euler deconcolution of gravity tensor gradiente data. Geophysics. 65(2):512-520.